Materials Research Express

RECEIVED
12 February 2019

REVISED
28 March 2019

ACCEPTED FOR PUBLICATION
9 April 2019

PUBLISHED
24 April 2019

PAPER

Study of GaAsSb:N bulk layers grown by liquid phase epitaxy for solar cells applications

M Milanova[1], V Donchev[2], K L Kostov[3], D Alonso-Álvarez[4], P Terziyska[5], G Avdeev[6], E Valcheva[2], K Kirilov[2] and S Georgiev[2]

[1] Central Laboratory of Applied Physics, 59 St. Petersburg blvd, 4000 Plovdiv, Bulgaria
[2] Faculty of Physics, Sofia University, blvd. James Bourchier, 5, 1164 Sofia, Bulgaria
[3] Institute of General and Inorganic Chemistry, Acad. Georgi Bonchev str., bl. 11, Bulgarian Academy of Sciences, 1113 Sofia, Bulgaria
[4] Department of Physics, Imperial College London, London, United Kingdom
[5] Institute of Solid State Physics, Bulgarian Academy of Sciences, 72, Tzarigradsko Chaussee, 1784 Sofia, Bulgaria
[6] Institute of Physical Chemistry, Acad. Georgi Bonchev str., bl. 11, Bulgarian Academy of Sciences, 1113 Sofia, Bulgaria

E-mail: vtd@phys.uni-sofia.bg

Keywords: liquid phase epitaxy, GaAsSb, GaAsSb(N), thick layers, optical properties, solar cells

Abstract

We present an original study of bulk epitaxial GaAsSb:N layers in view of photovoltaic applications of this material. The layers are grown on n-GaAs substrates by low-temperature liquid phase epitaxy (LPE). The grown GaAsSb:N layers exhibit reproducible properties and good optical quality. A number of experimental methods including x-ray diffraction, energy dispersive x-ray spectroscopy, atomic force microscopy, x-ray photoelectron spectroscopy and Raman spectroscopy are applied for investigation of the structural properties, surface morphology, local arrangement and chemical bonding of Sb and N in the obtained compounds. The band gap values at room temperature assessed from surface photovoltage and photoluminescence (PL) measurements are in good agreement and are ~20 meV lower than those of reference GaAsSb layers. PL spectra measured at different temperatures (10–300 K) show a very weak S-shape-like behaviour of the PL peak energy position indicating minimal carrier localization. The obtained results reveal the capacity of the LPE for growing bulk GaAsSb:N layers with good optical quality.

1. Introduction

During the last decade GaAs-based alloy systems such as GaAsN, GaAsBi, GaAsSb are intensively studied for long wavelength optoelectronics applications [1–8]. The incorporation a small quantity of nitrogen (N), antimony (Sb) or bismuth (Bi) into the crystal lattice causes large-scale bowing of the band gap. Quaternary alloys such as InGaAsN, GaAsSbN offer the possibility of independent tuning of the lattice constant and the energy bandgap, which creates an additional flexibility desired in many applications such as solar cells and photodetectors. Significant progress in application of these materials has been achieved in many optoelectronic devices based on QW structures, such as infrared lasers and vertical-cavity surface-emitting lasers (VCSELs) for telecommunications [8–10]. However, the growth of thick epitaxial layers involves many problems which are absent in the QW structures.

For many years most of the works have been focused on the InGaAsN alloy system [11–23]. Recently, an increasing interest appears to the growth of bulk GaAsSb and GaAsSbN [24–31]. The incorporation of the large size Sb substitutional atoms into GaAs results in bandgap narrowing and an increase of the lattice parameter. However, the compositional fluctuations in ternary GaAsSb compounds lead to the arising of localized states in the band gap, which greatly affect the optical properties of the semiconductor alloy. The incorporation of a small quantity of N into GaAsSb leads to a further reduction of the bandgap and a decrease of the lattice parameter. In this quaternary alloy system, variations in the Sb content affects the valence band offset while the N content primarily affects the conduction band offset. This makes it possible to tune the conduction band and valence

band offsets independently, while keeping the lattice matching to GaAs [24, 32]. However, similar to the other dilute nitrides, GaAsSbN suffers from reduced optical properties with respect to GaAs. In addition, its photovoltaic parameters are poorer as compared to those of InGaAsN. Usually the growth methods used for deposition of GaAsSbN and GaAsSb layers are molecular-beam epitaxy and metal-organic chemical beam epitaxy. To the best of our knowledge, there are no reports on GaAsSb:N grown by liquid-phase epitaxy (LPE). Investigations of LPE grown GaAsN and InGaAsN have been reported in [3, 15, 17, 33–35].

The purpose of our work is to obtain a material with lower band gap than GaAs using LPE growth, which could be applied for fabrication of solar cells with extended infrared photosensitivity compared to GaAs. Previously we have obtained [15–17] InGaAs(Sb)N bulk layers nearly lattice matched to GaAs with good structural and optical properties, but the red shift of the spectral sensitivity with respect to GaAs is about 100 meV. This is due to the low solubility of nitrogen and low incorporation efficiency into GaAs lattice during LPE growth. Significantly larger shift (about 160 meV) is achieved for GaAsSb layers, but their photoresponse is week. Adding nitrogen even in the ultradilute region improves the intensity of the photoresponse and slightly shifts (about 20 meV) it to the longer wavelengths. In this study we investigate LPE grown GaAsSb:N bulk layers in view of the application of this material in solar cells. The structural properties and local microstructure of the grown layers are investigated by means of different experimental methods. The optical quality and electronic band structure of the alloys are studied by photoluminescence (PL) measurements in the range 10–300 K and surface photovoltage (SPV) spectroscopy at room temperature.

2. Experiment

A series of GaAsSb:N layers were grown on n-type (100) GaAs:Si ($\sim 2 \times 10^{18}$ cm^{-3}) substrates in conventional LPE system using horizontal graphite piston boat technique. Because of the huge miscibility region [36, 37], the technological parameters are carefully chosen to obtain GaAsSb:N compounds without phase separation. The crystallization was carried out from Ga + 4.5 at% Sb solutions with 6 N purity of the solvent metals. Polycrystalline GaAs and GaN were used as sources of As and N, respectively. The N content in the melt was 0.5 at% for all growth experiments. The charged boat was annealed at 720 °C for 1 h under Pd-diffused ultra-pure hydrogen flow in order to homogenize the melt and to reduce the residual impurities. Epitaxial layers were deposited from initial epitaxy temperature 570 °C. The growth occurred from super-cooled melt at a cooling rate of 0.5 °C min^{-1} for 35–40 min. Epitaxial GaAsSb layers were also grown at the same growth conditions as reference samples.

High-resolution x-ray diffraction (XRD) was used for determination of the lattice parameter, mismatch and crystalline quality of the layers. The measurements were performed in the $\theta/2\theta$ geometry on an x-ray diffractometer (Empyrean PANalytical B.V., Holland) equipped with parallel beam optic, PIX cell detector and Cu Kα tube operated at a voltage of 45 kV and current of 45 mA. The Sb content of the GaAsSb:N samples was determined by energy dispersive x-ray spectroscopy (EDX) (Quantax, Bruker) to be ~3.4 at%. The same value was obtained for GaAsSb samples without nitrogen. The thickness of the layers was measured on cross sectional samples by scanning electron microscopy (SEM) (Tescan LYRA I XMU). The surface morphology was characterized by atomic force microscopy (AFM). The AFM topography image was obtained in soft tapping mode on a Quesant universal SPM apparatus. The AFM probe used was HQ:NSC19/Al BS (MikroMasch®) with cantilever force constant 0.5 N m^{-1} and resonance frequency 65 kHz, and tip radius ~8 nm.

In order to assess the chemical bonding and local microstructure in the GaAsSb:N alloys x-ray photoelectron spectroscopy (XPS) and micro-Raman spectroscopy were used. Raman spectra were recorded on a JobinYvon Lab RAM HR800 spectrometer with laser excitation of 632 nm in backscattering geometry at room temperature. The XPS experiments were carried out on AXIS Supra electron spectrometer (Kratos Analytical Ltd, a Shimadzu Group Company) with base vacuum in the analysis chamber of ~10^{-9} mbar. The spectra were measured using a double Al K_α/Mg K_α excitation source. The concentrations (in at%) of the observed chemical elements were calculated by normalizing the areas of the corresponding photoelectron peaks to their relative sensitivity factors. The procedure included also corrections for the differences in the transmission function and the inelastic mean free paths of the photo-emitted electrons with different kinetic energies. The accuracy of the binding-energy determination is within ±0.1 eV.

SPV spectra were recorded in the chopped light configuration [38] (94 Hz) applying the set-up and measurement procedure described elsewhere [39] and introducing a sheet of mica (15 μm) between the sample and the probe electrode. An AvaSpec-2048TEC Thermo-electric cooled Fiber Optic Spectrometer equipped with a Sony 2048 CCD light detector was used for quick PL measurements at room temperature exciting by a 532 nm laser with 20 mW. In addition, PL spectra at different temperatures were measured using laser excitation at 532 nm (Nd:YAG) with a power of 140 mW and a 0.5 m focal length spectrometer (Acton 2300i, Princeton Instruments) with a Si detector.

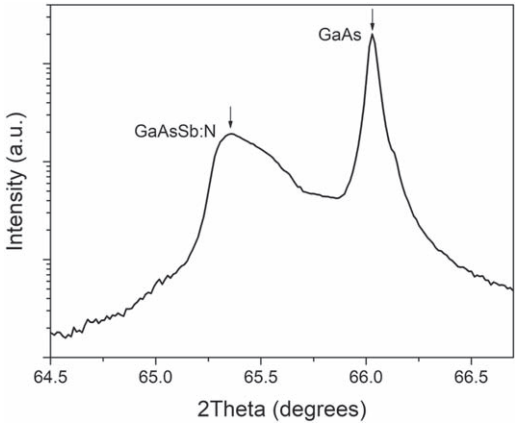

Figure 1. XRD theta/2theta diffraction curves of GaAsSb:N on GaAs around (004) reflections.

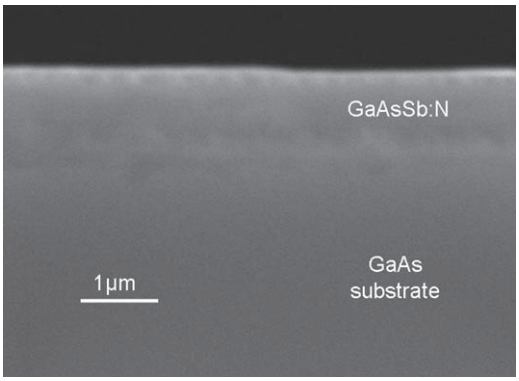

Figure 2. SEM image of the cross-section of a GaAsSb:N layer grown on GaAs substrate.

3. Results and discussion

3.1. Structural properties

3.1.1. XRD, SEM and AFM measurements

Figure 1 shows a typical high resolution XRD (004) scan spectrum of a GaAsSb:N/GaAs sample. The sharp peak corresponds to the GaAs substrate, while the signal from the GaAsSb:N layer is weaker and broader. The lattice mismatch $\Delta a/a_o$ determined from the distance between the XRD peaks is about 0.48%. The broad layer peak suggests relaxation of the metamorphic layer. Since the thicknesses of the epitaxial layers are about or higher than 1 micron (see below), we consider that they are nearly relaxed. Using the Sb composition measured separately by EDX ($x \approx 0.068$) and Vegard's rule (equation (1)) for the lattice constant of relaxed layers, the N content in the crystal lattice is estimated to be $y \approx 0.001$.

$$a(GaAs_{1-x-y}Sb_xN_y) = (1 - x - y) * a(GaAs) + x * a(GaSb) + y * a(GaN) \quad (1)$$

A cross-section SEM image of a GaAsSb:N epitaxial layer is shown in figure 2. The interface between substrate and layer is not smooth which is due to some mismatch between their lattice parameters as can be seen from the XRD measurements. The layers thicknesses measured on cross-sections of different samples are in the range 1.0–1.2 μm.

Figure 3 presents the AFM topography image of a GaAsSb:N layer surface. It shows undulated surface morphology formed as a result of the plastic relaxation in the metamorphic layer followed by surface step formation [40, 41]. The RMS roughness of the surface is 2.4 nm over the entire area of the image. N-induced nano-formations related to the peculiarity of the growth process are observed on the surface. In addition to the low solubility of nitrogen in the melt and in the solid these formations may further limit the incorporation of N in the layer.

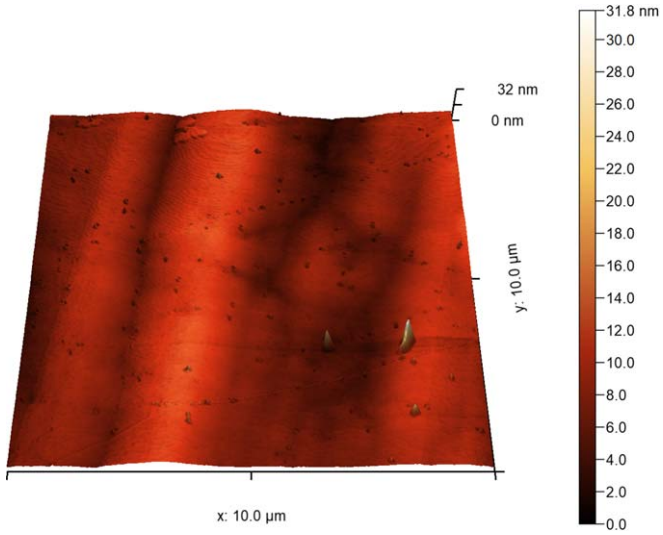

Figure 3. AFM surface topography image of a GaAsSb:N layer.

3.1.2. XPS measurements

The photoelectron spectra of GaAsSb:N show a complex structure of overlapping peaks, which requires the application of a deconvolution procedure. The fit parameters, especially the spin-orbital splitting of Ga 3d- and As 3d-doublets, have been determined measuring a GaAs standard by monochromatized Al K_α x-ray radiation. The surface chemical composition of the as-prepared GaAsSb:N sample shows a presence of thick layer containing mainly Sb- and Ga-oxides, and also traces of As-surface oxide. This oxide layer was fully removed, as well as part of the GaAsSb:N sample with thickness of ~90 nm after Ar^+ - ion bombardment with ion energy of 1 keV.

Photoelectron peaks of Ga 3d, Sb 4d and As 3d characterizing a clean GaAsSb:N sample are detected in the low binding-energy region displayed in figure 4(a). The corresponding $3d_{5/2}$ - peaks of Ga and As are observed at 19.0 eV and 40.9 eV while the binding-energy peaks at 31.7 eV and 32.9 eV can be attributed to $4d_{5/2}$ and $4d_{3/2}$ peaks of Sb incorporated in the GaAs lattice. The results are in good agreement with the literature data [42–45]. Note, that in XPS measurements the relative sensitive factors (RSFs) of Sb 4d- and Sb 3d-photoelectrons are significant higher than the RSFs of As 3d and Ga 3d electrons (and also of O 1s-electrons) which makes the detection of small amounts of antimony in GaAsSb:N reliable.

At a depth of about 90 nm from the surface, only single Sb $3d_{5/2}$ - and Sb $3d_{3/2}$ - peaks have been measured in the high binding-energy region (figure 4(b)) in agreement with the single Sb 4d-doublet observation in figure 4(a). The calculated concentration of the antimony atoms using the Sb 3d- or Sb 4d-peaks yield close results of 3.6 and 3.2 at%, respectively. These values correspond to the value found by EDX.

The use of Al K_α x-ray radiation does not lead to a reliable determination of the nitrogen content in GaAsSb:N because the N 1s peak is shielded by the substantially intense Ga $L_2M_{45}M_{45}$ Auger structure as can be seen in our previous study [17]. To address this problem we also used excitation with Mg K_α radiation resulting in the displacement of the Ga LMM structure to low binding-energies. Nevertheless, a weak and broad Ga Auger peak is also observed on the photoelectron background [46]. To distinguish the N 1s signal from this background, having in mind the very low nitrogen content in the GaAsSb:N sample, the experiment parameters-the pass-energy, x-ray flux and registration time-were increased, which leads to the substantial decrease of background noise. In addition, the GaAs standard was used for comparison purposes. The results for the GaAsSb:N and GaAs samples and their difference are shown in figure 4(c). A weak and noisy peak appears at about 398 eV in the difference spectrum that can be attributed to the N 1s peak of nitrogen atoms. This result allows us to confirm the presence of nitrogen in the studied samples, although a quantitative estimation of its concentration is difficult to achieve because the uncertainty of its calculation is very high in this region of weak signals measured at the limit of the detection sensitivity (around 0.1 at%).

3.1.3. Raman spectroscopy

Figure 5 shows Raman spectrum of a GaAsSb:N layer at room temperature. It consists of two GaAs - like sharp LO and TO lines and many week peaks over a large frequency range. Both LO and TO peak are red shifted in comparison with the phonon modes of GaAs influenced by the different material composition. They reveal significant reduction of the intensity of the GaAs like LO peak and an increase in intensity of the forbidden TO

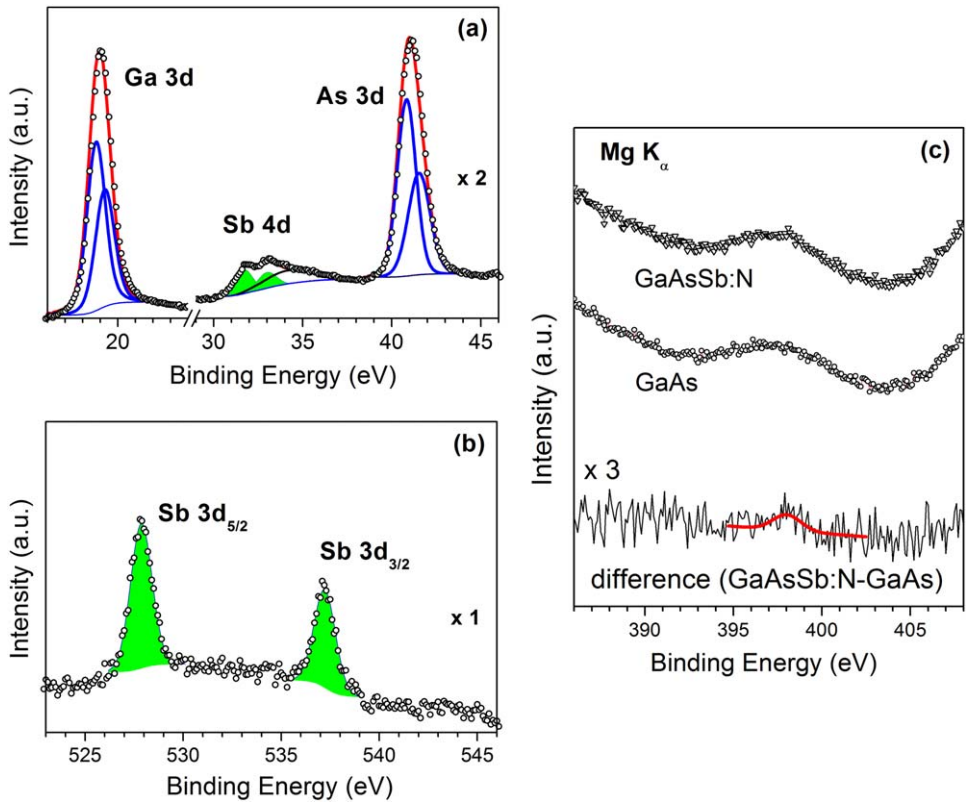

Figure 4. Photoelectron spectra of a GaAsSb:N sample after Ar^+- ion bombardment (with ion energy of 1 keV): (a) Ga 3d-, As 3d- and Sb 4d-photoelectron region; (b) Sb 3d-spectral region. The peak-fitting contributions and their sum are marked in blue and red, respectively. The Sb 4d- and Sb 3d- peak areas of antimony are coloured in green; (c) N 1s - photoelectron regions of the GaAsSb:N sample, GaAs standard and their difference (shown from top to bottom) recorded with Mg K_α excitation radiation. The fit of N 1s peak is marked in red.

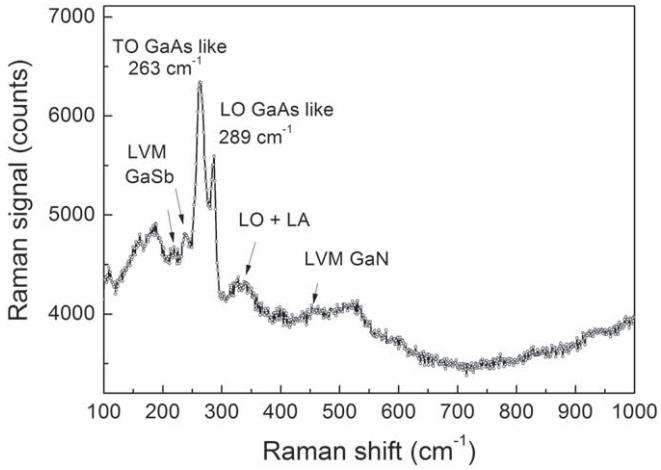

Figure 5. Raman spectrum of GaAsSb:N at room temperature.

peak. Additional two peaks around 220 and 240 cm^{-1} are also observed and could be associated with the local vibration mode (LVM) of GaSb in the GaAs lattice [47, 48]. The week peak at 454 cm^{-1} could be assigned to N induced LVM (as a result of N incorporation into the crystal lattice). Two peaks at 162 cm^{-1} and 188 cm^{-1} are observed also in the spectrum. Such peaks were reported for MBE grown and annealed GaAsSbN samples [27, 47]. The peaks at about 330 cm^{-1} could be assigned to a combination of LA and LO phonons [49]. Second order scattering of the GaAs peaks are observed over a frequency range between 500 and 550 cm^{-1}. All these observations clearly evidence the presence of some disorder. This is also in correspondence with the broad XRD peak indicative of nearly relaxed layers.

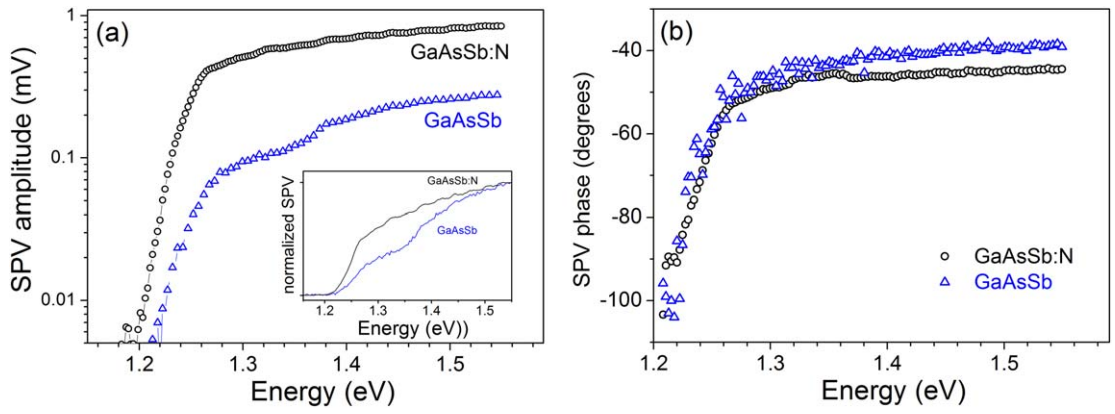

Figure 6. Typical SPV amplitude (a) and phase (b) spectra of GaAsSb:N (black circles) and GaAsSb (blue triangles) layers. The inset in (a) shows the normalized amplitude spectra in linear scale.

3.2. Optical properties

3.2.1. SPV spectroscopy

To study the optical absorption characteristics of the layers SPV spectra were measured. Figure 6 presents typical SPV amplitude and phase spectra of a GaAsSb and a GaAsSb:N layers. The SPV amplitude spectrum is considered as emulating the optical absorption [38]. The spectrum of GaAsSb:N shows larger signal by a factor, which increases from 3 for 800 nm to 6.5 for 1010 nm indicating better photo-response. Therefore adding nitrogen into GaAsSb even at ultradilute level, improves the photo-response of the material. The improvement is more pronounced for photon energies below the GaAs band-gap. This is also seen from the inset of figure 6(a), which presents the normalized SPV amplitude spectra of the two samples. The above observations could be explained as follows. The strain effects caused by Sb and N atoms are opposite in sign: Sb try to expand, while N try to shrink the crystal lattice. Therefore, N in small quantities leads to partially passivation of the Sb-related localized states in the band gap of GaAsSb and this way weakens the carrier trapping effects in the alloy. The step around 1.22 eV in figure 6(a) corresponds to the optical absorption edge. The band gap energy of GaAsSb:N assessed from Tauc plot is 1.24 eV, which is 180 meV lower than the band gap of GaAs (1.42 eV) and ~20 meV lower than that of the GaAsSb sample.

The SPV phase values of the two samples displayed in figure 6(b) are similar. They are in the 4th quadrant, which indicates that the bending of the energy bands across the structure is upward in the direction from the bulk towards the surface [39]. Such bending is expected at the interface layer-substrate because of the high n-type doping of GaAs. The upward band bending at the surface shows that the doping of the layers is also n-type [39].

3.2.2. PL measurements

Figure 7 presents typical PL spectra of a GaAsSb and a GaAsSb:N layers measured at room temperature. The spectra are similar in terms of shape, but the PL peak of GaAsSb:N is red shifted by ~20 meV with respect to that of GaAsSb in agreement with the SPV results. Applying the band-anticrossing model [50], this shift corresponds to a N content $y \approx 0.001$, which is in a good agreement with the XRD results. The PL peak position is considered as an estimate of the band gap energy. For the GaAsSb:N sample it is 1.23 eV.

The optical emission of GaAsSb:N layers is investigated also by means of temperature-dependent PL measurements. The normalized PL spectra measured in the temperature range between 10 and 300 K are presented in figure 8(a). For compounds of this kind (GaAsSb, GaAsN, GaAsSbN) the PL peak position commonly demonstrates a strong S-shape behavior with the temperature at low temperatures [30, 31, 34, 51, 52]. This behaviour is a characteristic of carrier localization effects induced by compositional fluctuations. At low temperatures, the carriers are trapped in Sb or N-related localized states. As the temperature increases, the carriers acquire enough thermal energy to escape out of the localized states and as a result, the PL peak energy initially increases. At even higher temperatures, it follows the expected decrease with temperature due to the band gap decrease. Figure 8(b) displays a very weak S-shape-like behavior of the PL peak energy with temperature. The latter follows quite well Varshni's formula $E_g(T) = E_0 - aT^2/(T + b)$ with $E_0 = 1.32$ eV, $a = 5 \times 10^{-4}$ eV.K^{-1} and $b = 276$ K. This indicates that the optimally chosen technological LPE growth conditions suppress the compositional fluctuations and hence minimize the carrier localization in the alloy.

For all samples, the PL peak full width of half-maximum increases with increasing the temperature, as expected. The integrated PL intensity decreases with increasing the temperature (figure 8(c)) due to the

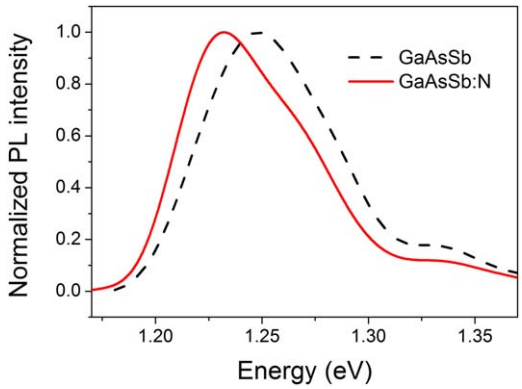

Figure 7. Room temperature PL spectra of GaAsSb (black dashed line) and GaAsSb:N (red solid line) layers.

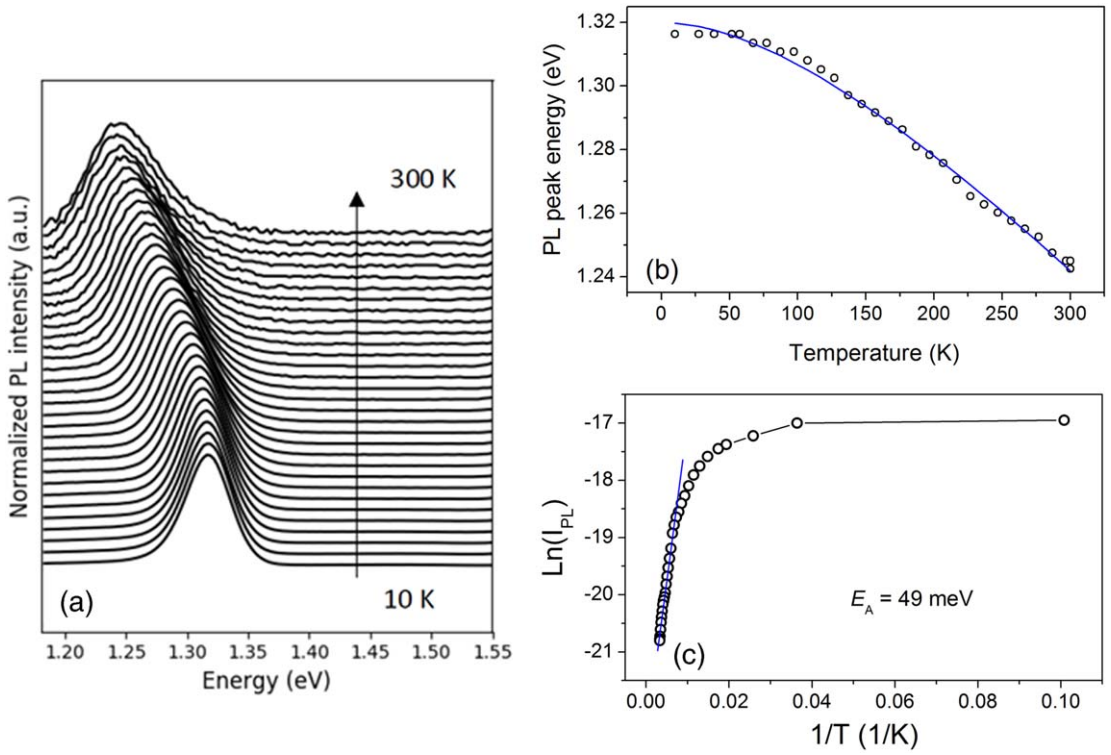

Figure 8. (a) PL spectra of GaAsSb:N measured at different temperatures between 10 and 300 K. (b) Temperature dependence of the PL peak energy position (symbols) fitted with Varshni's formula (line) with $E_0 = 1.32$ eV, $a = 5 \times 10^{-4}$ eV.K^{-1} and $b = 276$ K. (c) Ln of the integrated PL intensity as a function of the inverse temperature (symbols) and fit (line).

activation of non-radiative recombination channels. The estimate of the activation energy E_A obtained from Arrhenius plots of the Ln of the PL intensity versus the reciprocal absolute temperature is 49 meV. Similar values for E_A have been reported for quantum wells of GaAsSbN/GaAs (42–46 meV) [53] and GaAsN/GaAs (50 meV) [54] grown by molecular beam epitaxy and explained by the presence of N induced defects in the crystal lattice.

4. Conclusion

An original study is presented of bulk GaAsSb:N layers 1.0 μm thick grown on n-GaAs substrates by low-temperature LPE. The Sb composition $x \sim 0.068$ in the alloy is determined by EDX and confirmed by XPS measurements. The N composition evaluated from XRD measurements applying Vegard's rule is $y \sim 0.001$. The surface of the layer is slightly undulated because of the plastic relaxation with RMS surface roughness of the order of 2.4 nm, as found by AFM. The nitrogen and antimony bonding configurations have been studied by means of XPS and Raman spectroscopy. The XPS spectra reveal clearly the Sb content and give indication for the

presence of a weak N 1 s peak at ~398 eV corresponding to very low nitrogen concentration close to the detection limit, most probably around 0.1 at%. The Raman spectra reveal two sharp GaAs-like LO and forbidden TO peaks, and week LVM peaks connected with Sb and N incorporation in the GaAs lattice. SPV and PL measurements of the GaAsSb:N layers at room temperature reveal band gap values of good correspondence, which are about 20 meV lower than the band gap values of the reference GaAsSb layers with the same Sb content. PL spectra measured at different temperatures reveal negligible S-shape behaviour of the PL peak energy with temperature, which attest for minimal carrier localization at low temperatures due to the optimally chosen technological LPE growth conditions that suppress the compositional fluctuations. The SPV phase spectra indicate upward energy band bending at the layer surface and interface and n-type doping of the layer.

The obtained results reveal the capacity of the LPE method for growing GaAsSb:N as a promising material for photovoltaic applications. In this sense, they contribute to the searching of alternative ways for obtaining solar cells with higher efficiency.

Acknowledgments

This work was supported by the Cost Action MP1406 'Multiscale in modelling and validation for solar photovoltaics (MultiscaleSolar)' and the Bulgarian Ministry of Education and Science under the National Research Programme E+: Low Carbon Energy for the Transport and Households (grant agreement D01-214/2018). The authors acknowledge S. Russev for the EDX and SEM measurements and MikroMasch® for the AFM measurements.

ORCID iDs

V Donchev https://orcid.org/0000-0003-3812-4474

References

[1] Tisch U, Finkman E and Salzman J 2002 The anomalous bandgap bowing in GaAsN *Appl. Phys. Lett.* **81** 463
[2] Das S C and Dhar S 2011 Transport of nitrogen atoms during liquid phase epitaxial growth of InAsN and GaAsN *Semicond. Sci. Technol.* **26** 085025
[3] Milanova M, Kakanakov R, Koleva G, Arnaudov B, Evtimova S, Vitanov P, Goranova E, Bakardjieva V and Alexieva Z 2009 Incorporation of nitrogen in melt grown GaAs *J. Optoelectron. Adv. Mater.* **11** 1471–4 (http://joam.inoe.ro/download.php?idu=2125)
[4] Biswas M, Shinde N, Makkar R L, Bhatnagar A and Chakrabarti S 2017 Varying nitrogen background pressure; an efficient approach to improve electrical properties of MBE-grown GaAs1−xNx thin films with less atomic disorder *J. Alloys Compd.* **695** 3163–9
[5] Gelczuk Ł, Kopaczek J, Rockett T B O, Richards R D and Kudrawiec R 2017 Deep-level defects in n-type GaAsBi alloys grown by molecular beam epitaxy at low temperature and their influence on optical properties *Sci. Rep.* **7** 12824
[6] Rockett T B O, Richards R D, Gu Y, Harun F, Liu Y, Zhou Z and David J P R 2017 Influence of growth conditions on the structural and opto-electronic quality of GaAsBi *J. Cryst. Growth* **477** 139–43
[7] Jones C M and Kioupakis E 2017 Effect of strain on band alignment of GaAsSb/GaAs quantum wells *J. Appl. Phys.* **122** 045703
[8] Hossain N, Jin S R, Sweeney S J, Yu S-Q, Johnson S R, Ding D and Zhang Y-H 2010 Improved performance of GaAsSb/GaAs SQW lasers *Novel in-plane Semiconductor Lasers IX* ed A A Belyanin and P M Smowton (Washington, USA: SPIE) p 761608
[9] Tansu N and Mawst L J 2002 Temperature sensitivity of 1300-nm InGaAsN quantum-well lasers *IEEE Photonics Technol. Lett.* **14** 1052–4
[10] Lifang X, Patel D, Menoni C S, Yeh J-Y, Mawst L J and Tansu N 2012 Experimental evidence of the impact of nitrogen on carrier capture and escape times in InGaAsN/GaAs single quantum well *IEEE Photonics J* **4** 2262–71
[11] Hashimoto A, Kitano T, Nguyen A K, Masuda A, Yamamoto A, Tanaka S, Takahashi M, Moto A, Tanabe T and Takagishi S 2003 Raman characterization of lattice-matched GaInAsN layers grown on GaAs (001) substrates *Sol. Energy Mater. Sol. Cells* **75** 313–7
[12] Khan A, Kurtz S R, Prasad S, Johnston S W and Gou J 2007 Correlation of nitrogen related traps in InGaAsN with solar cell properties *Appl. Phys. Lett.* **90** 243509
[13] Aho A, Tommila J, Tukiainen A, Polojärvi V, Niemi T and Guina M 2014 Moth eye antireflection coated GaInP/GaAs/GaInNAs solar cell *AIP Conf. Proc.* **1616** 33–6 (https://aip.scitation.org/doi/abs/10.1063/1.4897022)
[14] Milanova M, Vitanov P, Terziyska P, Popov G and Koleva G 2012 Structural and electrical characteristics of InGaAsN layers grown by LPE *J. Cryst. Growth* **346** 79–82
[15] Donchev V, Milanova M, Asenova I, Shtinkov N, Alonso-Álvarez D, Mellor A, Karmakov Y, Georgiev S and Ekins-Daukes N 2018 Effect of Sb in thick InGaAsSbN layers grown by liquid phase epitaxy *J. Cryst. Growth* **483** 140–6
[16] Donchev V, Milanova M, Lemieux J, Shtinkov N and Ivanov I G 2016 Surface photovoltage and photoluminescence study of thick Ga(In)AsN layers grown by liquid-phase epitaxy *J. Phys.: Conf. Ser.* **700** 012028
[17] Milanova M, Donchev V, Kostov K L, Alonso-Álvarez D, Valcheva E, Kirilov K, Asenova I, Ivanov I G, Georgiev S and Ekins-Daukes N 2017 Experimental study of the effect of local atomic ordering on the energy band gap of melt grown InGaAsN alloys *Semicond. Sci. Technol.* **32** 085005
[18] Kurtz S R, Klem J F, Allerman A A, Sieg R M, Seager C H and Jones E D 2002 Minority carrier diffusion and defects in InGaAsN grown by molecular beam epitaxy *Appl. Phys. Lett.* **80** 1379–81
[19] Pavelescu E-M, Wagner J, Komsa H-P, Rantala T T, Dumitrescu M and Pessa M 2005 Nitrogen incorporation into GaInNAs lattice-matched to GaAs: the effects of growth temperature and thermal annealing *J. Appl. Phys.* **98** 083524

[20] Ptak A J, Friedman D J, Kurtz S and Kiehl J 2005 Enhanced-depletion-width GaInNAs solar cells grown by molecular-beam epitaxy *Conf. Record of the Thirty-first IEEE Photovoltaic Specialists Conf. (Lake Vuena Vista, Florida, 2005)* pp 603–6 (https://ieeexplore.ieee.org/document/1488203)
[21] Yamaguchi M *et al* 2008 Novel materials for high-efficiency III–V multi-junction solar cells *Sol. Energy* **82** 173–80
[22] Skierbiszewski C *et al* 2000 Large, nitrogen-induced increase of the electron effective mass in $In_yGa_{1-y}N_xAs_{1-x}$ *Appl. Phys. Lett.* **76** 2409–11
[23] Aho A, Korpijärvi V-M, Tukiainen A, Puustinen J and Guina M 2014 Incorporation model of N into GaInNAs alloys grown by radio-frequency plasma-assisted molecular beam epitaxy *J. Appl. Phys.* **116** 213101
[24] Braza V, Reyes D F, Gonzalo A, Utrilla A D, Ben T, Ulloa J M and González D 2017 Sb and N incorporation interplay in GaAsSbN/GaAs epilayers near lattice-matching condition for 1.0–1.16-eV photonic applications *Nanoscale Res. Lett.* **12** 356
[25] Roy D and Samajdar D P 2017 Analytical modeling and performance study of GaAsNSb based single junction solar cell lattice matched to GaAs substrate for use in tandem solar cells *Sol. Energy* **158** 483–9
[26] Hsu H-P, Lin Y-T and Lin H-H 2012 Evidence of nitrogen reorganization in GaAsSbN alloys *Jpn. J. Appl. Phys.* **51** 22605
[27] Bharatan S, Iyer S, Nunna K, Collis W J, Matney K, Reppert J, Rao A M and Kent P R C 2007 The effects of annealing on the structural, optical, and vibrational properties of lattice-matched GaAsSbN／GaAs grown by molecular beam epitaxy *J. Appl. Phys.* **102** 023503
[28] Lin Y-T, Ma T-C, Chen T-Y and Lin H-H 2008 Energy gap reduction in dilute nitride GaAsSbN *Appl. Phys. Lett.* **93** 171914
[29] Chen C-K, Ma T-C, Lin Y-T and Lin H-H 2008 GaAsSbN/GaAs long wavelength PIN detectors *2008 20th Int. Conf. on Indium Phosphide and Related Materials (Versailles, France, 2008)* pp 1–4 (https://ieeexplore.ieee.org/document/4703012)
[30] Gao X *et al* 2017 Effect of rapid thermal annealing on the optical properties of GaAsSb alloys *Opt. Mater. Express* **7** 1971–9
[31] Gao X *et al* 2016 Investigation of localized states in GaAsSb epilayers grown by molecular beam epitaxy *Sci. Rep.* **6** 29112
[32] Ulloa J M, Reyes D F, Montes M, Yamamoto K, Sales D L, González D, Guzman A and Hierro A 2012 Independent tuning of electron and hole confinement in InAs/GaAs quantum dots through a thin GaAsSbN capping layer *Appl. Phys. Lett.* **100** 13107
[33] Dhar S, Halder N, Kumar J and Arora B M 2004 Observation of a 0.7 eV electron trap in dilute GaAsN layers grown by liquid phase epitaxy *Appl. Phys. Lett.* **85** 964–6
[34] Bhuyan S, Das S K, Dhar S, Pal B and Bansal B 2014 Optical density of states in ultradilute GaAsN alloy: coexistence of free excitons and impurity band of localized and delocalized states *J. Appl. Phys.* **116** 023103
[35] Dhar S, Mondal A and Das T D 2008 Hall mobility and electron trap density in GaAsN grown by liquid phase epitaxy *Semicond. Sci. Technol.* **23** 015007
[36] Gratton M F and Woolley J C 1980 Investigation of two- and three-phase fields in the Ga-As-Sb system *J. Electrochem. Soc.* **127** 55
[37] Stringfellow G 1982 Miscibility gaps in quaternary III/V alloys *J. Cryst. Growth* **58** 194–202
[38] Kronik L and Shapira Y 1999 Surface photovoltage phenomena: theory, experiment, and applications *Surf. Sci. Rep.* **37** 1–206
[39] Donchev V, Ivanov T, Germanova K and Kirilov K 2010 Surface photovoltage spectroscopy—an advanced method for characterization of semiconductor nanostructures *Trends Appl. Spectrosc.* **8** 27–66
[40] Andrews A M, Speck J S, Romanov A E, Bobeth M and Pompe W 2002 Modeling cross-hatch surface morphology in growing mismatched layers *J. Appl. Phys.* **91** 1933–43
[41] Yan J Y, Gong Q, Yue L, Liu Q B, Cheng R H, Cao C F, Wang Y and Wang S M 2013 Growth of metamorphic InGaP layers on GaAs substrates *J. Cryst. Growth* **378** 141–4
[42] Ghosh S C, Biesinger M C, LaPierre R R and Kruse P 2007 X-ray photoelectron spectroscopic study of the formation of catalytic gold nanoparticles on ultraviolet-ozone oxidized GaAs(100) substrates *J. Appl. Phys.* **101** 114322
[43] Suri R, Lichtenwalner D J and Misra V 2010 Interfacial self cleaning during atomic layer deposition and annealing of HfO_2 films on native (100)-GaAs substrates *Appl. Phys. Lett.* **96** 112905
[44] Ghita R V, Negrila C, Manea A S, Logofatu C, Cernea M and Lazarescu M F 2003 X-ray Photoelectron Spectroscopy Study on n-Type GaAs *J. Optoelectron. Adv. Mater.* **5** 859–63 (https://joam.inoe.ro/arhiva/pdf5_4/Ghita.pdf)
[45] Reiche R, Holgado J P, Yubero F, Espinos J P and Gonzalez-Elipe A R 2003 Characterization of Sb_2O_3 subjected to different ion and plasma surface treatments *Surf. Interface Anal.* **35** 256–62
[46] Moulder J F, Stickle W F, Sobol P E, Bomben K D and Chastain J 1992 *Handbook of X-ray Photoelectron Spectroscopy: A Reference Book of Standard Spectra for Identification and Interpretation of XPS Data* ed J Chastain (Flying Cloud Drive, United States of America: Perkin-Elmer Corporation, Physical Electronics Division)
[47] Bharatan S, Iyer S, Matney K, Collis W J, Nunna K, Li J, Wu L, McGuire K and McNeil L E 2005 Growth and properties of lattice matched GaAsSbN epilayer on GaAs for solar cell applications *MRS Proc.* **891** 0891–EE10
[48] Ahmad E, Karim M R, Bin H S, Reynolds C L, Liu Y and Iyer S 2017 A two-step growth pathway for high Sb incorporation in GaAsSb nanowires in the telecommunication wavelength range *Sci. Rep.* **7** 10111
[49] Sekine T, Uchinokura K and Matsuura E 1976 Two-phonon Raman scattering in GaSb *Solid State Commun.* **18** 1337–40
[50] Lin Y T, Ma T C, Chen T Y and Lin H H 2008 Energy gap reduction in dilute nitride GaAsSbN *Appl. Phys. Lett.* **93** 1–4
[51] Lourenço S A, Dias I F L, Duarte J L, Laureto E, Aquino V M and Harmand J C 2007 Temperature-dependent photoluminescence spectra of GaAsSb/AlGaAs and GaAsSbN/GaAs single quantum wells under different excitation intensities *Brazilian J. Phys.* **37** 1212–9
[52] Lai F-I, Kuo S Y, Wang J S, Kuo H C, Wang S C, Wang H S, Liang C T and Chen Y F 2006 Effect of nitrogen contents on the temperature dependence of photoluminescence in InGaAsN／GaAs single quantum wells *J. Vac. Sci. Technol.* A **24** 1223–7
[53] Lourenço S A, Dias I F L, Poças L C, Duarte J L, De O J B B and Harmand J C 2003 Effect of temperature on the optical properties of GaAsSbN/GaAs single quantum wells grown by molecular-beam epitaxy *J. Appl. Phys.* **93** 4475–9
[54] Buyanova I A, Chen W M, Monemar B, Xin H P and Tu C W 2000 Photoluminescence characterization of GaNAs/GaAs structures grown by molecular beam epitaxy *Mater. Sci. Eng.* B **75** 166–9